3.4 Mass production of organic nanocrystals

The reprecipitation method is an easy and convenient technique to fabricate organic nanocrystals in general. However, only limited amount of nanocrystals dispersion (about several-tens ml) was prepared at once, i.e. the laboratory scale. To overcome this problem, we introduced a pump as an injection apparatus of the reprecipitation method for mass-production of pigment nanocrystals with controlled size and morphology (Ujiiye-Ishii et al., 2006).

For mass-production, most efficient conditions of the reprecipitation method have injecting highly concentrated solution with high injection rate. The former condition was achieved by using 1-methyl-2-pyrrolidone (NMP) and the latter was realized by using a high flow-rate pump. Using the injection pump-assisted reprecipitation method, the amount of obtained quinacridone nanocrystals in dispersion was 700 mg per minute at maximum, and then 3.5 g of the nanocrystals were obtained in one experiment. This value was about 17,500 times

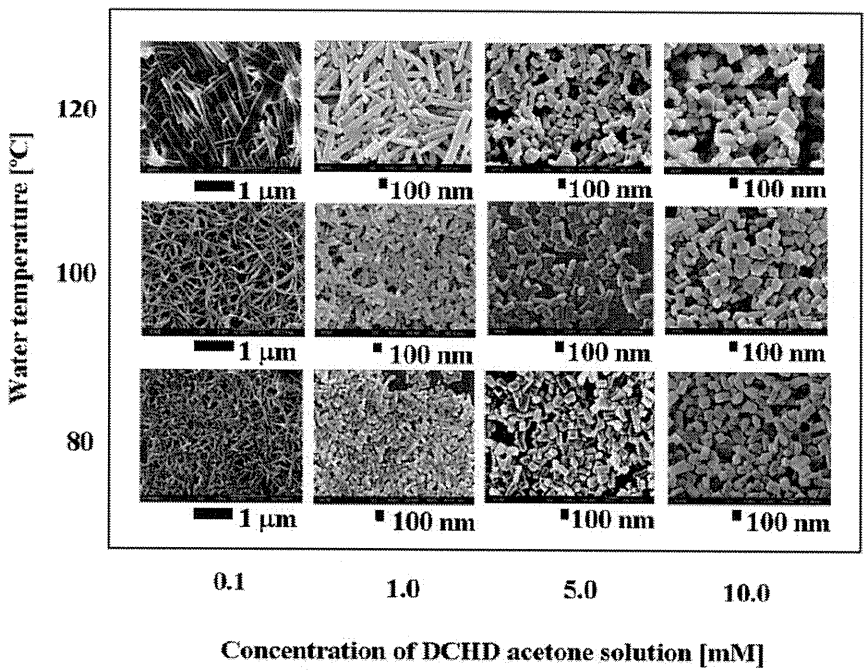

Fig. 5. Poly(DCHD) nanocrystals prepared by the closed-type microwave-irradiation reprecipitation method. (Reprinted from (Baba, et al., 2007a): Japanese Journal of Applied Physics. Vol. 46 (2007) pp. 7558-7561, No. 11, DOI: 10.1143/JJAP.46.7558. Copyright 2007 The Japan Society of Applied Physics)

larger than that obtained by the conventional reprecipitation method with manual injection. The size of quinacridone nanocrystals fabricated was 25–80 nm, which was confirmed by observation using a scanning electron microscope. From the powder X-ray diffraction data, only α-type nanocrystals were obtained. This mass production procedure of pigment nanocrystals is useful for an application of a color filter.

4. Several functional organic nanocrystals

4.1 Color filter using organic pigment nanocrystals

Organic pigments have been widely used in printing and coating industries as the coloring agents of synthetic fibers and plastics. Recent years, some organic pigments have an attention as organic photoconductors such as organic EL materials and electrophotographic photoreceptors. In addition, organic pigments are used for ink-jet inks to produce photographic-quality pictures and for color filters that are essential materials for the full-colorization of digital cameras and liquid crystal displays (LCDs). To increase the performance of the color filter, it is absolutely essential to cancel out the light scattering by reducing the particle size of organic pigments. Yet dyes can be an attractive alternative to overcome this limitation due to the reduced light scattering because they are dissolved in the media and exist in molecule form, however, in order for the dyes to be applied successfully to LCDs manufacturing process, their low thermal stability needs to be improved. Therefore, as the way to reduce the particle size, the breakdown method using beads and/or inorganic salts are commonly used. However, an energy efficiency, inclusion of contaminants such as bead materials (e.g., inorganic salts and zirconia), and a difficulty to reduce the particle size less than 50 nm are causing industrial problems. Therefore, the solution of these problems has been strongly desired. To overcome these problems, mass production procedure of organic pigment nanocrystals by the newly developed reprecipitation method was investigated, and the possibility of their application to color filter for LCDs was evaluated.

To evaluate the prepared organic pigment nanocrystals as a functional material for color filters, it is necessary to significantly increase their preparation amount. For this realization, a highly concentrated pigment solution and an improvement in the injection rate of the solution were necessary. Based on the literature (Ujiiye-Ishii et al., 2006), the system using a pulsation-free pump was built. In this newly developed reprecipitation method, it increased the preparation amount of nanocrystals by 104–106 times (Miyashita et al., 2008).

The organic pigment nanocrystals prepared by the reprecipitation method were finer in mono-dispersed property, compared to the conventional products. The average size of pigment nanocrystals prepared by the reprecipitation method was 25 nm and that of the pigments prepared by the breakdown improved milling method was 39 nm, and the former was in finer size dispersion (i.e., mono-dispersion). The relationship between the particle formation mechanism and particle size in the reprecipitation method is also under study. To clarify the reduction of the light scattering that is affected by the reduced size of pigment particles, the light scattering intensity was measured using a goniometer. In LCDs, if the light scattering occurs by pigment particles, the reduction of the display contrast and/or the luminance ratios occurs. Thus this becomes a serious problem when the display is in ON/OFF in LCDs.

It is apparent that the use of pigment nanocrystals prepared by the reprecipitation method can significantly increase the contrast ratio of LCDs, which is one of the most important performances. As a result, a new production process of organic pigment nanocrystals reduced the light scattering by fine size and well dispersed organic pigment nanocrystals prepared by the reprecipitation method.

It was found that organic pigment nanocrystals with the particle size about 25 nm were successfully achieved by the reprecipitation method. Because the fine size-controlled organic pigment nanocrystals lead to very little light scattering, they are considered to be useful for improving the performance of color filters that are an essential component of LCD.

4.2 Organic nanocrystals for organic field effect transistor

The functionality of organic pigment is attracted in electro devices such as organic electro luminescence devices and organic field effect transistor (OFET). Especially, the research of OFET is hot topic toward a future of optical device. Several kinds of electron-hole transfer organic compounds are well investigated. For OFET, carrier mobility is important factor for high quality devices. A π-conjugate polymer, polydiacetylene (PDA), is one of the promising compounds having high carrier mobility. PDA is a unique material, which combine the properties of an essentially one-dimensional, fully conjugated polymer with the ability of single crystalline monomers to polymerize without disruption of the crystallinity (Takahashi, et al., 2002). PDA has the optical properties of large non-linear optical susceptibility and ultra-fast response time as well as a PDA been predicted to present very high charge carrier mobility, up to 10^3–10^5 cm^2/V s. However the real mobility of PDA crystals measured using time-of-flight technique was found to be 1–10 cm^2/V s, and that is comparable to those measured on polyacene molecular crystals such as anthracene or naphthalene. The use of PDA films as an active layer of OFET is very promising task, however the pure electrical conductivity of these films have restricted their application. Thus to improve the conductivity is attracted work. Several attempts to improve the electrical conductivity have been reported; chemical doping into the stage of monomer crystals and in the course of solid-state polymerization, chemical doping into soluble polydiacetylenes, chemical doping into a Langmuir–Blodgett film of PDA, ion implantation to PDA bulk crystals, and using a scanning tunneling microscopy probe tip to fabricate linear PDA nanowires. Recently, the maximum conductivity for chemically doped PDA crystals has been reported to be as high as 10^{2} S/cm. As a widely held opinion, one of the big issues in increasing the conductivity of PDA is that its rigid crystalline lattice prevents the dopant from penetrating into PDA bulk crystals. This was especially the case in 1,6-di-*N*-carbazolyl-2,4-hexadiyne (DCHD).

To overcome the difficulty of chemical doping to PDA, we tried chemically doping into the nanocrystals of PDA, because PDA nanocrystals are known to have a softened crystal lattice (Baba, et al., 2006) and a large surface area, compared with bulk crystals, and demonstrated almost the highest conductivity of chemically doped PDA ever reported (Baba, et al., 2008). Figure 6 shows that the single layered poly-DCHD nanocrystals on slide glass and their specimen for measuring their conductivity. The success in chemical doping was achieved because poly-DCHD nanocrystals have a large surface area and softened crystal lattices, which allows chemical dopant species to diffuse easily into poly-DCHD nanocrystals in good contrast to the case of bulk crystals. Actually, nanostructure showed unique conformation change during solid state polymerization. Nanostructure have showed crack-less action during polymerization. This also showed that the nanocrystal has softened crystal lattice and has flexible stricture (this is mentioned in the next section). Thus, the PDA nanocrystals can accept the dopant. Aiming at the fully doped single crystalline nanocrystals of PDA, the effects of crystal size, morphology, and several kinds of chemical dopant species, which would increase the conductivity of PDA, are now under investigation.

As future approach, achieving the one dimensional array of the PDA nanofibers layered on the surface of devices is promising approach for high conductivity. We previously reported the one dimensional array of nanofibers. Furthermore, interesting finding concerning morphology changes during solid-state polymerization of PDA nanofibers were reported by our group, which related to topochemical study. This was because the softened crystal lattice of nanocrystals.

4.3 Solid state polymerization of polydiacetylene: topochemical polymerization

The research of the topochemical polymerization has been reported extensively since the 1960s, and PDA is the most attracted one. PDA also has been attracted because this π-conjugated polymer system has received much attention as conductive and non-linear optical materials. However, the accumulation of strain in bulk crystal during the solid-state

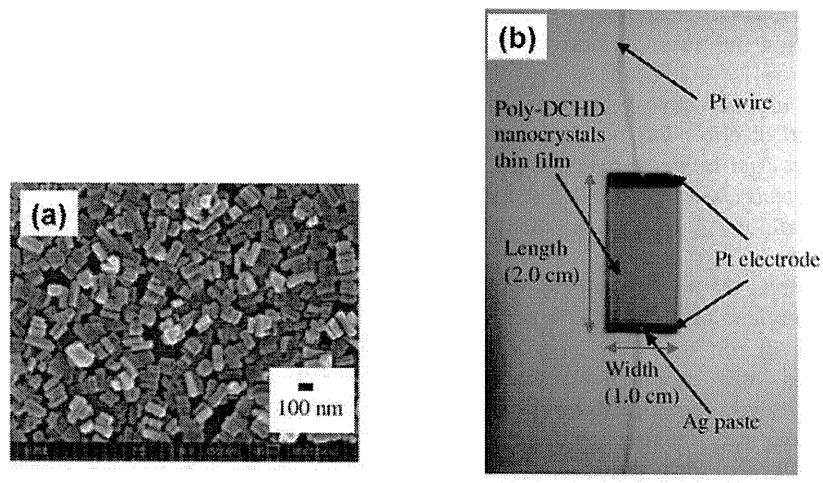

Fig. 6. (a) Single layered poly(DCHD) nanocrystals on quartz slide glass. (b) Image of the specimen for conductivity measurement of single layered poly(DCHD) nanocrystals. (Reprinted from (Baba, et al., 2008): Japanese Journal of Applied Physics., Vol. 47 (2008), pp. 3769-3771, No. 5, DOI: 10.1143/JJAP.47.3769. Copyright 2008 The Japan Society of Applied Physics)

polymerization results in crushing crystal structure, and the rate of polymeric conversion does not occur with high efficiency. We found that the polymerization of nanocrystals achieved high quality polymeric crystal because the strain accumulated in nanocrystals was easily released (Baba, et al, 2006). Nanofibers prepared by the reprecipitation method had an average length of 10 μm and width of 50 nm. We found interesting behavior of morphological change of nanofibers during the stage of the solid-state polymerization. DCHD monomer nanofibers, which were fabricated by the reprecipitation method, were worm-like before solid-state polymerization. Interestingly, worm-like nanofibers converted into straight-like ones through the solid-state polymerization. This phenomenon indicated that the lattice in nanofibers was generally soft, compared with that of bulk crystals. The crystalline nanofibers are useful for the estimation of a nonlinear optical property and a conductivity of a single polymer chain.

4.4 Linear and nonlinear optical property of organic nanocrystals

PDA crystals have attractive nonlinear optical properties. Our interest is the nonlinearity occurred in nanocrystals. The fabrication of polydiacetylene nanocrystals with varied size was achieved using the reprecipitation method. The size effect on the absorption spectra, which was a characteristic to organic nanocrystals, has been experimentally verified. An

important point is that size-dependent blue-shift appears at a size an order of magnitude larger than that of semiconductors and metals. That is due to the lattice vibration must become highly frequent with increasing temperature and also with decreasing crystal size. Actually, these thermal effects and sizes were clearly related to phonons in the nanocrystals lattice. The obtained $\chi^{(3)}$ was the order of 10^{-9} esu (Nakanishi & Katagi, 1998). Thus, we believe PDA nanocrystals is promising NLO materials. These attractive data was obtained in two-dimensional structured thin films of polymer matrix. Further our interest was constructing the three-dimensional (3-D) structure of nonlinear materials such as photonic crystals.

Photonic crystals have been a subject of considerable interest for more than a decade. A great deal of effort has been put into preparing highly ordered photonic crystals for the visible spectral range. Initial studies were directed toward the linear optical properties of these crystals, but more recent studies have focused on nonlinear processes in photonic crystals, and dramatic enhancements of these properties have been reported (Markowicz, et al., 2004).

Our interest is to study the optical properties of highly ordered 3-D arrays of polydiacetylene nanocrystals, since 3-D arrays formed by mono-dispersed particles in the range of 10 nm to 1 μm, referred to as colloidal crystals, show some special optical properties and potential applications, particularly in photonic devices. However, polydiacetylene nanoparticles are usually polyhedral and multi-dispersed. Their morphology prevents them from forming large-scale densely packed 3-D structures because the particles that form colloidal crystals are required to have a size variation of less than 5%. Polystyrene is one of the important materials in the fabrication of colloidal crystals, since uniform spherical polystyrene particles were easily synthesized by soap-free emulsion polymerization. When polydiacetylene nanocrystals are enclosed within uniform spherical polystyrene particles, the resulting composite particles are used to construct 3-D arrays of nonlinear materials. We reported the fabrication and characterization of spherical mono-dispersed composite particles consisting of 1,6-di(*N*-carbazolyl)-2,4-hexadiyne (DCHD) nanocrystals cores and polystyrene shells. We succeeded in preparing mono-dispersed composite particles consisting of poly-DCHD cores and polystyrene shells (Wei, et al., 2003). Their 3-D structure is attractive for investigating their nonlinear optical properties.

Recently, an interest of photonic crystals has also been directed toward studying the effect of disorder in photonic crystals. Prasad's group reported on a type of disorder in photonic crystals in which only a random variation of refractive index is introduced, without creating any structural or positional disorder, which was referred to be such disordered photonic crystals as photonic crystal alloys (Tiryaki, et al., 2004). The vertical deposition colloidal crystal method to produce three-dimensional photonic crystal alloys of polystyrene and poly(methyl methacrylate), 300 nm spheres in varying compositions were used. This photonic crystal alloys provided a convenient medium to compositionally tune the bandgap and the wavelength of a phase-matched nonlinear optical response. Prasad's group is saying that the use of photonically active components (such as dye-doped spheres) allows one to conveniently create microcavities and study cavity electrodynamics.

4.5 Nanomedicine: Drug delivery system using drug nanocrystals

Numerous commonly used pharmaceutical drugs are hydrophobic in nature. Thus, special formulations are required to make their aqueous dispersion for these drugs delivery.

Usually, surfactants or other nanoparticle-based delivery vehicles are used. Once systemic administration of these drugs, if the drug target cancer organ, such drug-doped carriers are preferentially taken up by tumour tissues based on the "enhanced permeability and retention effect". The carriers include liposomes, polymeric micelles, oil dispersions (micelles), ceramic, hydrophilic drug–polymer complexes and polymeric nanoparticles. However many surfactants themselves tend to increase the systemic toxicity of the drug formulation. Therefore, there is increasing interest in the development of novel drug formulation and delivery methods without any external agents such as surfactants or other carrier vehicles. One method proposed for dispersion of hydrophobic compound in water, the reprecipitation method was used as demonstration.

Prasad's group have prepared the nanocrystal formulation of a hydrophobic drug for photodynamic therapy (PDT) and compared its efficacy with the conventional surfactant-based formulation (Baba, et al., 2007b). PDT is a promising new modality for the treatment of a variety of cancers and some dermatological and ophthalmic diseases. The main advantage of PDT is the capability to localize the treatment, by using selective light exposure to the tumor site. Typical PDT treatment involves systemic administration of a photosensitizer drug, then localized light exposure at the tumor site using near-infrared light. After being excited with light, these photosensitizer molecules can transfer their excited-state energy to molecular oxygen in the surroundings, forming reactive oxygen species such as singlet oxygen. The locally generated reactive oxygen species destruct various cellular compartments, resulting in irreversible damage to tumor cells. The major disadvantage for successful clinical PDT is the poor water solubility of photosensitizing drugs. Thus, making their stable formulation for systemic administration is highly challenging. To overcome this difficulty, a stable dispersion of these drugs into aqueous systems is achieved using delivery vehicles. However, allergic reactions and their sustained *in vivo* toxicities are caused by the carrier vehicles. Therefore, the ideal formulation for safe and efficient PDT should involve the minimal number of additional agent such as carrier. To overcome these problems, nanocrystals, which were monodispersed with diameter 100 nm (ζ-potential: −40 mV), were prepared by the reprecipitation method (Baba, et al., 2007b).

There was interesting finding that though the fluorescence and photodynamic activity of the drug nanocrystals were initially quenched in aqueous media. However, both recovered under *in vitro* and *in vivo* conditions (Baba, et al., 2007b). This recovery of drug activity and fluorescence was attributed to the interaction of nanocrystals with blood serum or other intracellular components (e.g., serum albumin), resulting in conversion of the drug nanocrystals into the molecular form. Efficacy of the nanocrystals formulation *in vitro* and *in vivo* was found to be comparable with that of the same drug formulated in the conventional delivery vehicle.

These results have not only mentioned the potential of using pure drug nanocrystals for PDT, but also this approach eliminates the need of any external agents such as surfactants or other carrier vehicles for drug delivery. Further studies are expected to increase the efficacy of nanocrystals by controlling their size that may affect long-term *in vivo* circulation and accumulation in the tumor tissue. Potentially, this method of drug formulation can be applied not only for PDT drugs, but also for delivery of other therapeutic drugs including imaging agents such as fluorescent dyes for biophotonics (e.g., bioimaging).

4.6 Bioimaging using fluorescent dye nanocrystals

Fluorescence microscopy is one of the most versatile imaging techniques in biomedical research. That allows the non-invasive imaging of cells and tissues with molecular specificity. Such imaging requires a fluorescent dye to enter cells and tissues prior to visualization. Currently used dyes include members of the coumarin, rhodamine, fluorescein, and carbocyanine families. One of them, 3,3′-Dioctadecyloxacarbocyanine perchlorate [DiO; DiOC18(3)] is the long-chain dialkylcarbocyanine dye, and most commonly used for the visualization of anterograde and retrograde neuronal tracers in living cells. This lipophilic carbocyanine is also employed in many other applications, including cytotoxicity assays, the labeling of lipoproteins, and the tracking of cell migration and lipid diffusion in membranes through fluorescence recovery after photobleaching. The hydrophobic nature of these dyes means that, in many cases, organic solvents [e.g., dimethylformamide, dimethylsulfoxide (DMSO)] and surfactants are required for successful cell imaging. However, unfortunately, organic solvents and surfactants themselves tend to increase cytotoxicity *in vitro* and *in vivo*. On the other hand, the direct applications of micron-sized crystals have also been investigated, although such crystals are probably not small enough to allow the diffusion of dyes into cells, i. e. not efficient imaging approach.

In addition to DiO dyes, many other fluorescent dyes are hydrophobic in nature—including perylene, a widely studied hydrophobic material that functions with a high quantum yield in organic electroluminescence devices. Although it is potentially useful for bioimaging, the preparation of aqueous dispersions of perylene dyes requires special formulation techniques, similar to those for DiO. The reprecipitation method was used to solvent-free and non-invasive bioimaging. We reported an organic solvent-free bioimaging method employing fluorescent dye nanocrystals prepared using the reprecipitation method and their application to *in vitro* fluorescence confocal imaging (Baba et al., 2009, 2010).

These nanocrystal formulations allowed efficient fluorescence confocal imaging of living cells *in vitro*, with performances almost identical to those obtained by treatment using a conventional organic solvent. This nanocrystal formulation approach to *in vitro* bioimaging in cultures eliminates the need for external solubilizing agents (e.g., organic solvent or surfactant), which usually tend to increase cytotoxicity. We expect that this method can be used with a wide range of hydrophobic organic fluorophores. As an advanced functional bioimaging tool, our team recently have developed thermoresponsive fluorescent nanocrystals, which will be useful for temperature-dependent cell imaging as well as photodynamic cancer therapy.

4.7 Thermoresponsive behaviour of fluorescent organic nanocrystals

After the first introduction of a temperature-responsive polymer, poly(*N*-isopropylacrylamide) (PNIPAM) (Heskinsa & Guillet, 1968), numerous studies on this polymer have been reported. The fundamental findings have been applied in various fields such as drug delivery, regenerative medicine, (Nishida, et al., 2004) and analytical chemistry. The property of this polymer is that when the temperature of the aqueous solution where the polymer is dissolved increases above the lower critical solution temperature of the cloud point, the polymer shows phase separation. The hydrophobic groups in the polymer form insoluble aggregates, turning the solution cloudy (Chen & Hoffman, 1995). Using this characteristic of PNIPAM, fluorescent dyes covalently linked to PNIPAM showed on-off fluorescent switching properties above and below the critical

temperature. On the other hand, we demonstrated the thermoresponsive behaviour of fluorescent organic nanocrystals using PNIPAM in an aqueous system for the first time (Baba, et al., 2011). For the preparation of thermoresponsive fluorescent organic nanocrystals, fluorescent dyes of perylene, quinacridone, and zinc phthalocyanine were used. As a result, an on-off switching of fluorescence intensity was observed below and above around cloud point (~35°C). This thermoresponsive behaviour of fluorescent organic nanocrystals in the aqueous system was stably repeatable. As an extension of this research, this research finding indicates that the fluorescence properties of organic nanocrystals can be controlled using the phase-transitional functional polymer system, where the key factors for stimulation are not only limited to temperature but also light and pH. This fundamental finding of tuneable fluorescence optical property of organic nanocrystals will have several applications such as thermosensitive fluorescence bioimaging of living cells/tissues using PNIPAM-based fluorescent dye nanocrystals; the on-off switching logic gate for optical devices; and medical treatment by photodynamic therapy using PNIPAM-based on-off switching photosensitizing nanocrystals, where the drug efficacy can be controlled by temperature on demand. We believe this finding will be applied in multidisciplinary fields such as nanomedicine, nanobiology, tissue engineering, regenetic medicine, and applied optical physics.

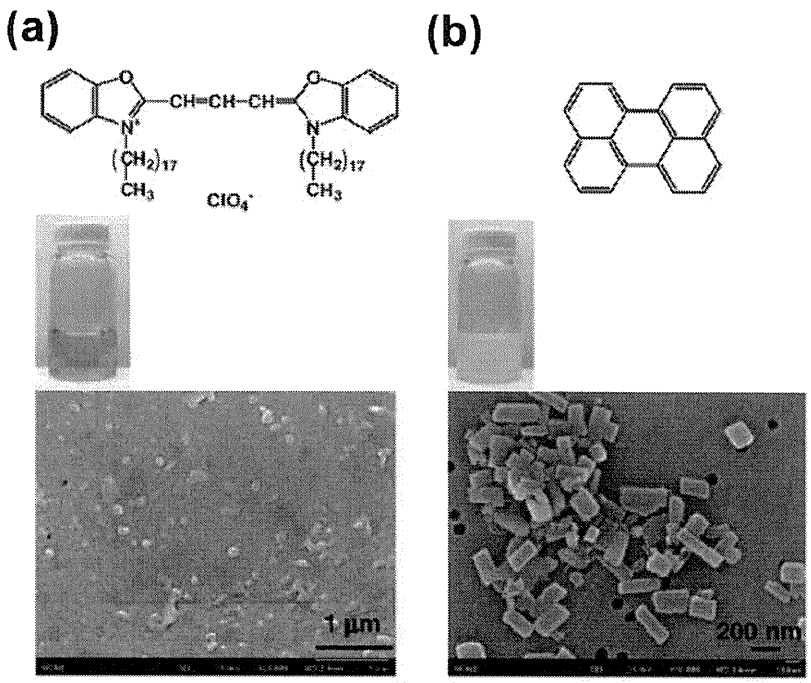

Fig. 7. Chemical structure, photographs of dispersion, SEM images of (a) DiO and (b) perylene. (Reprinted from (Baba, et al., 2009): Japanese Journal of Applied Physics. Vol. 48 (2009), 117002 (4 pages), DOI: 10.1143/JJAP.48.117002. Copyright 2009 The Japan Society of Applied Physics)

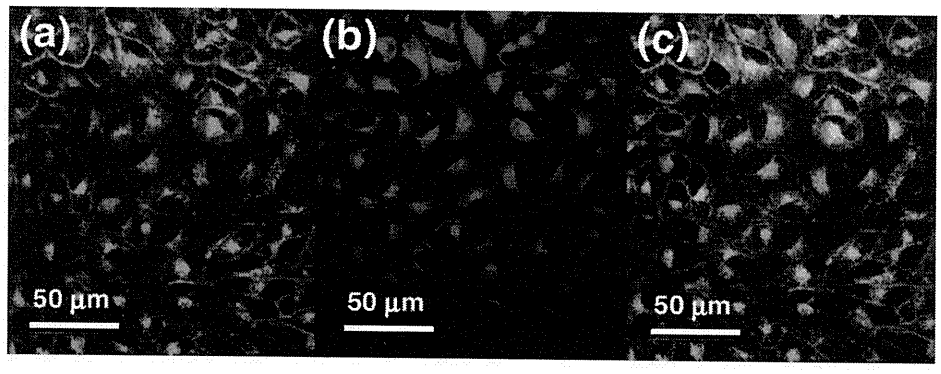

Fig. 8. Confocal fluorescence images of culture cells *in vitro*. Dyes used for the staining are (a) DiO and (b) perylene. (c) Double staining image that is overlapped pictures of (a) and (b). (Reprinted from (Baba, et al., 2009): Japanese Journal of Applied Physics. Vol. 48 (2009), 117002 (4 pages), DOI: 10.1143/JJAP.48.117002. Copyright 2009 The Japan Society of Applied Physics)

5. Recent topics of organic nanocrystals achieved by several groups

Now a day, with using the reprecipitation method, a series of functional organic nanocrystals/nanoparticles were successfully fabricated by several research groups. For example, nanocrystals from perylene and a perylene derivative were prepared and the spectroscopies of single nanoparticles were studied. Nanoparticles were prepared from β-carotene and observed the influence of both supramolecular structure and particle size on the absorption spectra. The size dependence of the luminescence and the enhanced emission of the nanoparticles prepared with this method were studied in Yao's group (Fu & Yao, 2001) and Park's group (An, et al., 2002). One of the interesting feature occurred in

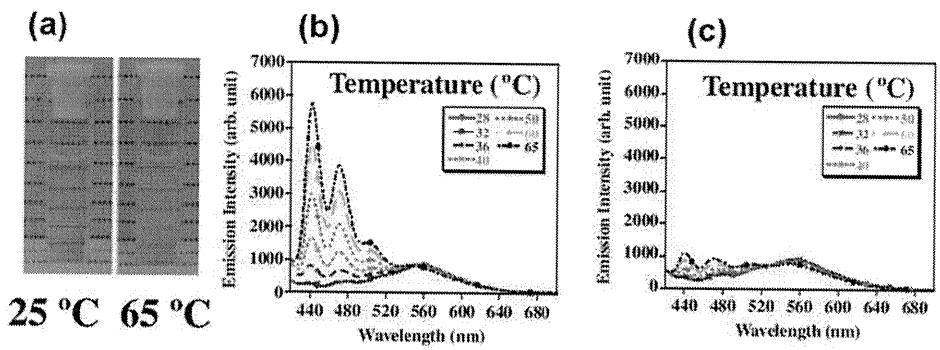

Fig. 9. (a) Photographs of perylene nanocrystals dispersion with PNIPAM at 25 (left) and 65 °C (right). Fluorescence spectra of the nanocrystals (b) with and (c) without PNIPAM. (Reprinted from (Baba, et al., 2011): Japanese Journal of Applied Physics. Vol. 50 (2011), 010202 (3 pages), DOI: 10.1143/JJAP.50.010202. Copyright 2011 The Japan Society of Applied Physics)

nanocrystals, recently Park' group reported a phenomenon named aggregation induced enhanced emission (AIEE). Here, enhanced emission instead of fluorescence quenching was observed in the solid state for some specific fluorophores. In general, the fluorescence efficiency of organic chromophores decreases in the solid state, as a result of concentration quenching, even though they show high fluorescence efficiency in solution. Park's group reported AIEE from organic nanoparticle. First, Park's group synthesized the organicmolecule 1-cyano-trans-1,2-bis-(40-methylbiphenyl)ethylene (CN-MBE), and then prepared the corresponding nanoparticles. It was interesting that although the fluorescent from CN-MBE solution was quite weak, the nanoparticles emitted a quite strong photoluminescence. It was considered that the aggregation induced the planarization of the CN-MBE molecules in the nanoparticles, which in turn resulted in the strong intermolecular interactions causing a specific aggregation that was good for efficient emission. This phenomenon was specific to nanoparticles and not to bulky crystals.

Not only the above mentioned optical properties, but also some other optoelectronic properties of organic nanomaterials have been reported in recently. For example, the electronic conductance through organic nanowires was investigated. The Tetracyanoquinodimethane (TCNQ) charge transfer complexes nanowires and field emission properties of tris(8-hydroxyquinolino)-aluminum (Alq 3) nanowires were reported. The field-effect transistors (FETs) based on single-crystalline organic one-dimensional nanomaterials were fabricated, and also lasers have proved to be another promising application for organic one-dimensional nanomaterials. The optical waveguiding properties of organic nanowires were reported. The details are well reviewed in the literature written by Yao's group (Zhao, et al., 2008).

6. Conclusion

In this chapter, first we explained the preparation method of organic nanocrystals and their improved ones. The reprecipitation method is very useful technique for fabricating several kinds of functional organic nanocrystals. Supercritical fluid crystallization method, microwave-irradiation method, and mass production method extend the potential of the reprecipitation method. Then, several kinds of functional organic nanocrystals including recent topics achieved by several research groups were introduced. The research trend of functional organic nanocrystals had begun with a series of optoelectronic materials, and recently several functional organic nanocrystals were revealed to be useful for nanomedicine such as drug delivery system using pure nanocrystal form of drugs as well as organic solvent free confocal fluorescence imaging of living cells *in vitro*. The unique finding of thermoresponsive behaviour of fluorescent organic nanocrystals will be quite useful for bioimaging, regenetic medicine, applied optics, etc. Toward the future works of functional organic nanocrystals, their basic research and application will much more extend to the fields such as optelectronic materials, applied optics as well as nanomedicine, regenetic medicine, and biophotonics.

7. References

An, B.-K.; Kwon, S.-K.; Jung, S.-D. & Park, S. Y. (2002). Enhanced emission and its switching in fluorescent organic nanoparticles. *Journal of the American Chemical Society*. Vol. 124, No. 48, (November 8, 2002), pp. 14410-14415, ISSN 0002-7863

Baba, K.; Kasai, H.; Okada, S.; Oikawa, H. & Nakanishi, H. (2000). Novel fabrication process of organic microcrystals using microwave-irradiation. *Japanese Journal of Applied Physics*, Vol. 39, No. 12A, (October 16, 2000), pp. L1256-L1258, ISSN 0021-4922

Baba, K.; Kasai, H.; Okada, S.; Nakanishi, H. & Oikawa, H. (2006). Fabrication of diacetylene nanofibers and their dynamic behavior in the course of solid-state polymerization. *Molecular Crystals and Liquid Crystals*, Vol. 445, pp. 161-166, ISSN: 1542-1406

Baba, K.; Kasai, H.; Masuhara, A.; Okada, S.; Oikawa, H. & Nakanishi, H. (2007a). Diacetylene nanowire crystals prepared by reprecipitation/microwave-irradiation method. *Japanese Journal of Applied Physics*, Vol. 46, No. 11, (November 6, 2007), pp. 7558-7561, ISSN 0021-4922

Baba, K.; Pudavar, H. E.; Roy, I.; Ochulchanskyy, T. Y.; Chen, Y.; Pandey, R. K. & Prasad, P. N. (2007b). New method for delivering a hydrophobic drug for photodynamic therapy using pure nanocrystal form of the drug. *Molecular Pharmaceutics*, Vol. 4, No. 2, (February 1, 2007), pp. 289-297, ISSN 1543-8384

Baba, K.; Kasai, H.; Shinohara, Y.; Okada, S.; Oikawa, H. Matsuda, H. & Nakanishi, H. (2008). Chemical doping into nanocrystals of poly(diacetylene). *Japanese Journal of Applied Physics*, Vol. 47, No. 5, (May 16, 2008), pp. 3769-3771

Baba, K.; Kasai, H.; Masuhara, A.; Oikawa, H. & Nakanishi, H. (2009). Organic solvent-free fluorescence confocal imaging of living cells using pure nanocrystal forms of fluorescent dyes. *Japanese Journal of Applied Physics*, Vol. 48, No. 11 (November 20, 2009), pp. 117002/1-117002/4

Baba, K.; Kasai, H.; Nishida, K. & Nakanishi, H. (2010). Organic Nanocrystals for Nanomedicine and Biophotonics, In: *Nanocrystals*, M. Yoshitake, (Ed.), pp. 311-326, Sciyo, ISBN 978-953-307-126-8, Vukovar, Croatia

Baba, K.; Kasai, H.; Nishida, K. & Nakanishi, H. (2011). Poly(*N*-isopropylacrylamide)-based thermoresponsive behavior of fluorescent organic nanocrystals. *Japanese Journal of Applied Physics*, Vol. 50, (January 5, 2011), pp. 010202/1-010202-3

Chen, G. & Hoffman, A. S. (1995). Graft copolymers that exhibit temperature-induced phase transitions over a wide range of pH. *Nature*, Vol. 373, No. 6509, (05 January 1995), pp. 49-52, ISSN 0028-0836

Fu, H. & J. Yao, J. (2001). Size effects on the optical properties of organic nanoparticles. *Journal of the American Chemical Society*, Vol. 123, No. 7, (January 23, 2001), pp. 1434-1439, ISSN 0002-7863

Granqvist, C. G. & Buhrman, R. A. (1976). Ultrafine metal particles. *Journal of Applied Physics*, Vol. 47, No. 5, (May, 1976), pp. 2200-2219

Heskinsa, M. & Guillet, J. E. (1968). Solution properties of poly(N-isopropylacrylamide). *Journal of Macromolecular Science, Chemistry*, Vol. 2, Issue 8, pp. 1441-1455, ISSN 0022-233X

Ishizaka, T.; Kasai, H.; Oikawa, H. & Nakanishi, H. (2006). Unique luminescence properties of Eu3+-doped polyimide. *Journal of Photochemistry and Photobiology, A: Chemistry*, Vol. 183, Issue 3, (25 October 2006) pp. 280-284, ISSN: 1010-6030

Kaneko, Yuji; Shimada, Satoru; Fukuda, Takashi; Kimura, Tatsumi; Yokoi, Hiroyuki; Matsuda, Hiro; Onodera, Tsunenobu; Kasai, Hitoshi; Okada, Shuji; Oikawa, Hidetoshi & Nakanishi, H. (2005). A novel method for fixing the anisotropic

orientation of dispersed organic nanocrystals in a magnetic field. *Advanced Materials*, Vol. 17, Issue 2, pp. 160-163, ISSN: 0935-9648

Kasai, H.; Nalwa, H. S.; Oikawa, H.; Okada, S.; Matsuda, H.; Minami, N.; Kakuta, A.; Ono, K.; Mukho, A. & Nakanishi, H. (1992). A novel preparation method of organic microcrystals. *Japanese Journal of Applied Physics*, Vol. 31, No. 8A, (May 29, 1992), pp. L1132-L1134, ISSN 0021-4922

Kasai, H.; Kanbara, H.; Iida, R.; Okada, S.; Matsuda, H.; Oikawa, H. & Nakanishi, H. (1995). Optical Kerr shutter response of organic microcrystals. *Japanese Journal of Applied Physics*, Vol. 34, No. 9B, (August 11, 1995), pp. L1208-L1210, ISSN 0021-4922

Kasai, H.; Kamatani, H.; Okada, S.; Oikawa, H.; Matsuda, H. & Nakanishi, H. (1996). Size-dependent colors and luminescences of organic microcrystals. *Japanese Journal of Applied Physics*, Vol. 35, No. 2B, (January 8, 1996), pp. L221- L223, ISSN 0021-4922

Katagi, H.; Kasai, H.; Okada, S.; Oikawa, H.; Komatsu, K.; Matsuda, H.; Liu, Z. F. & Nakanishi, H. (1996). Size control of polydiacetylene microcrystals. *Japanese Journal of Applied Physics*, Vol. 35, 10B, (August 28, 1996), pp. L1364-L1366, ISSN 0021-4922

Komai, Y.; Kasai, H.; Hirakoso, H.; Hakuta, Y.; Okada, S.; Oikawa, H.; Adschiri, T.; Inomata, H.; Arai, K. & Nakanishi, H. (1998). Size and form control of titanylphthalocyanine microcrystals by supercritical fluid crystallization method. *Molecular Crystals and Liquid Crystals*, Vol. 322, (01 November 1998), pp. 167-172, ISSN 1058-725X

Markowicz, P. P.; Tiryaki, H.; Pudavar, H. & Prasad, P. N. (2004). Dramatic enhancement of third-harmonic generation in three-dimensional photonic crystals. *Physical review letters*, Vol. 92, No. 8, (26 February, 2004), pp. 083903, ISSN 0031-9007

Matsuda, H., Okada, S., Masaki, A., Nakanishi, H., Suda, Y., Shigehara, K. & Yamada, A. (1990). Molecular structural view on the large third order nonlinearity of phthalocyanine derivatives, *Proceedings of SPIE*, Vol. 1337, pp. 105-113, San Diego, CA, USA, (1 December, 1990)

Matsui, A.; Mizuno, K.; Nishi, O.; Matsushima, Y. & Shimizu, M. (1995). Densities of states and bandwidths of excitons in anthracene microcrystallites embedded in PMMA. *Chemical Physics*, Vol. 194, No. 1, (May 1, 1995), pp. 167-174, ISSN 0301-0104

Miyashita, Y.; Baba, K.; Kasai, H.; Nakanishi, H. & Miyashita, T. (2008). A new production process of organic pigment nanocrystals. *Molecular Crystals and Liquid Crystals*, Vol. 492, pp. 268-274, ISSN: 1542-1406

Murray, C. B.; Morris, D. J. & Bawendi M. G. (1993). Synthesis and characterization of nearly monodisperse CdE (E = sulfur, selenium, tellurium) semiconductor nanocrystallites. *Journal of the American Chemical Society*, Vol. 115, No. 19, (March 22, 1993), pp. 8706-8715, ISSN 0002-7863

Nakamura, A.; Tokizaki, T.; Akiyama, H. & Kataoka, T. (1992). Quantum size effects and optical nonlinearity of confined excitons in semiconducting microcrystallites. *Journal of Luminescence*, Vol. 53, No. 1-6, (July 1992), pp. 105-109, ISSN 0022-2313

Nakanishi, H. & Katagi, H. (1998). Microcrystals of polydiacetylene derivatives and their linear and nonlinear optical properties. *Supramolecular Science*, Vol. 5, Issue 3-4, pp. 289-295

Nishida, K.; Yamato, M.; Hayashida, Y.; Watanabe, K.; Yamanoto, K.; Adachi, E.; Nagai, S.; Kikuchi, A.; Maeda, N.; Watanabe, H.; Okano, T. & Tano, Y. (2004). Corneal reconstruction with tissue-engineered cell sheets composed of autologous oral mucosal epithelium. *The New England Journal of Medicine*, Vol. 351, No. 12, (September 16, 2004), pp. 1187-1196, ISSN 0028-4793

Takahashi, S.; Miura, H.; Kasai, H.; Okada, S.; Nakanishi, H. & Oikawa, H. (2002). Single-crystal-to-single-crystal transformation of diolefin derivatives in nanocrystals. *Journal of the American Chemical Society*, Vol. 124, No. 37, (August 24, 2002), pp. (10944-10945), ISSN 0002-7863

Tan, Z.; Masuhara, A.; Kasai, H.; Nakanishi, H. & Oikawa, H. (2008). Multibranched C_{60} micro/nanocrystals fabricated by reprecipitation method. *Japanese Journal of Applied Physics*, Vol. 47, Issue 2, Pt. 2, pp. 1426-1428

Tiryaki, H.; Baba, K.; Markowicz, P. P. & Prasad, P. N. (2004). Linear and nonlinear optical studies in photonic crystal alloys. *Optics Letters*, Vol. 29, No. 19, (October 1, 2004), pp. 2276-2278, ISSN 0146-9592

Ujiiye-Ishii, K.; Baba, K.; Wei, Z.; Kasai, H.; Nakanishi, H.; Okada, S. & Oikawa, H. (2006). Mass-production of pigment nanocrystals by the reprecipitation method and their encapsulation. *Molecular Crystals and Liquid Crystals*, Vol. 445, pp. 177-183, ISSN 1542-1406

Ung, T.; Giersig, M.; Dunstan, D. & Mulvaney, P. (1997). Spectroelectrochemistry of colloidal silver. *Langmuir*, Vol. 13, No. 6, (March 19, 1997), pp. 1773-1782, ISSN 0743-7463

Wei, Z.; Miura, H.; Masuhara, A.; Kasai, H.; Okada, S. & Nakanishi, H. (2003). Monodispersed poly diacetylene-polystyrene composite particles. *Japanese Journal of Applied Physics*, Vol. 42, No. 10A, (October 1, 2003), PP. L1213-L1215

Yanagawa, T.; Kurokawa, Y.; Kasai, H. & Nakanishi, H. (1997). Degenerate four-wave mixing using an optical parametric oscillator as an incoherent light source. *Optics Communications*, Vol. 137, Issue 1-3, (15 April 1997), pp. 103-106, ISSN 0030-4018

Zhao, G.; Ishizaka, T.; Kasai, H.; Hasegawa, M.; Furukawa, T.; Nakanishi, H. & Oikawa, H. (2009). Ultralow-dielectric-constant films prepared from hollow polyimide nanoparticles possessing controllable core sizes. *Chemistry of Materials*, Vol. 21, (29 December, 2008), pp. 419-424, ISSN 0897-4756

Zhao, Y. S.; Fu, H.; Peng, A.; Ma, Y.; Xiao, D. & Yao, J. (2008). Low-dimensional nanomaterials based on small organic molecules: preparation and optoelectronic properties. *Advanced Materials*, Vol. 20, No. 15, (4 JUL 2008) pp. 2859-2876, ISSN 0935-9648

Journal of Controlled Release 153 (2011) 278–287

Contents lists available at ScienceDirect

Journal of Controlled Release

journal homepage: www.elsevier.com/locate/jconrel

A method for enhancing the ocular penetration of eye drops using nanoparticles of hydrolyzable dye

Koichi Baba [a,b,*,1], Yuji Tanaka [b], Akira Kubota [b], Hitoshi Kasai [c,d], Shunji Yokokura [b], Hachiro Nakanishi [c], Kohji Nishida [a,b,1]

[a] Department of Advanced Ophthalmic Medicine, Tohoku University Graduate School of Medicine, 1-1 Seiryo, Aoba-ku, Sendai 980-8574, Japan
[b] Department of Ophthalmology and Visual Sciences, Tohoku University Graduate School of Medicine, 1-1 Seiryo, Aoba-ku, Sendai 980-8574, Japan
[c] Institute of Multidisciplinary Research for Advanced Materials, Tohoku University, 2-1-1 Katahira, Aoba-ku, Sendai 980-8577, Japan
[d] PRESTO, Japan Science and Technology Agency, 4-1-8 Honcho, Kawaguchi, Saitama 332-0012, Japan

ARTICLE INFO

Article history:
Received 15 November 2010
Accepted 17 April 2011
Available online 23 April 2011

Keywords:
Ocular penetration
Nanoparticles
Eye drops
Hydrolysis
Confocal laser fluorescence microscopy

ABSTRACT

This report describes a method for enhancing the ocular penetration of eye drops using nanoparticles of hydrolyzable dye, which is similar to a prodrug approach. The entry of eye drops into the ocular globe is restricted predominantly by corneal barrier functions. The barrier functions are epithelial tight junctions as well as a physicochemical property consisting of the opposite characteristics of a lipophilic epithelium and a hydrophilic stroma. We found that using a formulation of nanoparticles of hydrolyzable dye (with particles of 200 nm in diameter on average) attained a greater than tenfold higher (about 50-fold) ocular penetration than that of micron-sized particles. The nanoparticles were prepared by a carrier-free technique; i.e., the reprecipitation method. Confocal laser fluorescence microscopy showed that dyes originating from the nanoparticles surmounted the corneal epithelium barrier, which has tight junctions, and achieved deeper penetration into the cornea. The high penetration rate of the dyes into the cornea was attributed to the size of particles (i.e., nanoparticles) and a transformation of dye polarity from lipophilic to hydrophilic in *in vivo* hydrolysis reactions. We concluded that utilizing *in vivo* hydrolysis reactions to alter the physicochemical nature of nanoparticles consisting of hydrolyzable compounds was an effective approach for enhancing the ocular penetration of eye drops.

1. Introduction

A drug passing through tissue-specific barriers (e.g., blood–brain barrier, epidermal barrier or corneal barrier) is expected to reach targeted diseased organs. Current studies on designing adequate formulations of drugs to penetrate such barriers are of interest in medicine, pharmacy, chemistry and nanotechnology [1–5]. Enhancement of ocular penetration of eye drops remains one of the most challenging tasks in ophthalmology [6–9]. The majority of ophthalmic formulations are administered as eye drops because of their ease of use, low invasiveness and the simplicity with which such drugs can be formulated [6,7]. However, the anatomy, physiology and biochemistry of the eye form a unique structure that restricts the entry of drug molecules at the required site of action [10–12]. Most of the drug is washed out from the ocular surface by various mechanisms (e.g., lacrimation, tear dilution and tear turnover) before they are able to penetrate into the desired tissue [11]. Furthermore, the specific barrier that exists in the cornea strictly restricts the entry of the drugs remaining on the ocular surface. Eventually, less than 5% of the administered drug penetrates the cornea to reach intraocular tissues [13].

The cornea is a transparent membrane located in the central part of the ocular surface and is mainly composed of three layers: epithelium, stroma, and endothelium (schematic images of an eye and a cornea are shown in Supplementary Information, Fig. S1) [14]. A corneal epithelium is a stratified cell membrane and its apical tight junctions between surface epithelial cells are considered to be the most prominent barrier for corneal absorption. A corneal stroma is a hydrated fibrous tissue with dispersed cells and it has a hydrophilic environment limiting the penetration of highly lipophilic compounds. A corneal endothelium is a monolayer of cells with large intercellular junctions, which presents a leaky lipophilic barrier. Due to the dual nature of the cornea, with a lipophilic epithelium and a hydrophilic stroma, the epithelium appears to be rate limiting to the movement of hydrophilic compounds, whereas for lipophilic compounds, the stroma is rate limiting [15]. Thus, an epithelium and a stroma, which present different physicochemical properties, act as a strong

* Corresponding author at: Department of Ophthalmology, Osaka University Graduate School of Medicine, 2-2 Yamadaoka, Suita, Osaka 565-0871, Japan. Tel.: +81 6 6879 3456; fax: +81 6 6879 3458.
E-mail address: koichi.baba@ophthal.med.osaka-u.ac.jp (K. Baba).
[1] Department of Ophthalmology, Osaka University Graduate School of Medicine, 2-2 Yamadaoka, Suita, Osaka 565-0871, Japan.

0168-3659/$ – see front matter © 2011 Elsevier B.V. All rights reserved.
doi:10.1016/j.jconrel.2011.04.019

barrier to the entry of drugs into the ocular globe via the cornea [12,16–18].

At present, using the hydrolysis reaction that converts a drug polarity from lipophilic/hydrophobic to hydrophilic is a widely employed strategy to enhance drug penetration through the cornea, and such drugs are referred to as prodrugs [2]. Prodrugs are drugs with attached functionalities to obtain favorable structural natures and they regenerate their active parent form by enzymatic or chemical reactions [12].

One of the attractive approaches for increasing ocular drug penetration is using nanoparticles. Even though the lipophilic/hydrophobic drug molecule itself is not soluble in water, it can be regarded as showing water solubility by means of forming nanoparticles in aqueous medium with stable water dispersion [4,19]. Furthermore, an advantage of a nanoparticle formulation is the expected increase in ocular drug penetration based on a small particle size. For example, increased ocular drug penetration is expected by means of decreasing the particle size of a steroid, which has less water solubility, resulting in micron-sized sedimentation in currently used drug formulations [20,21]. Thus, in an effort to improve the quality of aqueous dispersion of lipophilic/hydrophobic drugs, there has been increasing interest in developing smaller sized particles.

Nanocarrier based approaches, which are useful for increasing the water solubility of lipophilic and hydrophobic drugs by containing these drugs within capsule carriers, are being widely investigated at present [13,19,22–24]. These approaches also allow for site specific targeting in drug delivery. However, nanocarriers, such as the nanosphere, liposome, and micelle, may lead to cytotoxicity and show insufficient drug levels or the uncontrolled release of drugs [25–29]. Furthermore, nanocarriers are not always ideal for increasing the ocular penetration of drugs [30]. Recently, the use of nanocarrier-free organic nanocrystals for photodynamic cancer therapy and bioimaging was reported, where stable water dispersion and high nanocrystal tissue uptake was achieved [31,32]. The nanocrystals were prepared by the reprecipitation method [31,32].

This article demonstrates a method for enhancing eye drop ocular penetration using nanoparticles of hydrolyzable dye. The nanoparticles were prepared by the reprecipitation method [31–33]. The two beneficial aspects of the nanoparticles are small size, which is expected to support stable water dispersion and high ocular penetration, and dye polarity transformation from lipophilic to hydrophilic in *in vivo* hydrolysis reactions, which may overcome the corneal barrier consisting of a lipophilic epithelium and hydrophilic stroma, which is similar to a prodrug approach. Thus, the nanoparticles are presented in this study as a candidate for the production of superior eye drops with stable water dispersion, nanocarrier-free status, and deeper ocular penetration.

As a model compound for demonstrating this concept, a hydrolyzable lipophilic dye, fluorescein diacetate (FDA), was selected. FDA is a non-fluorescent, non-polar fatty acid ester that is membrane permeable and can enter the cell [34]. FDA is hydrolyzed by esterases to produce hydrophilic fluorescein, a fluorescent compound that tends to accumulate intracellularly [34]. We selected FDA for this study because FDA is a lipophilic compound and is thus nearly water insoluble [35,36]. Also, FDA is suitable for fabricating nanoparticles based on the precipitation procedure in water by means of the reprecipitation method. Furthermore, FDA has been widely used for biological applications and the fluorescein it produces is currently used for ocular diagnostic treatments. Another advantage is that the resulting fluorescein dye can be used as a useful fluorescent tracer to determine the depth of ocular penetration. The final factor in the selection of FDA was the fact that FDA eye drops, including their fluorescein derivatives, can be administered to rats without producing abnormal behaviors.

We investigated whether FDA nanoparticle eye drops can penetrate through the corneal epithelium, which has tight junctions that usually act as a strong barrier to keep foreign substances from entering the ocular globe. We also determined whether they can overcome the physicochemical property barrier consisting of a lipophilic epithelium and a hydrophilic stroma. Nanoparticle eye drops were administrated to rats for qualitative observation by fluorescence microscopy and confocal laser fluorescence microscopy as well, as quantitative analysis. The nanoparticles and micron-sized FDA particles were compared with investigate the effect of particle size. Comparison was also made between FDA and its fluorescein derivatives to assess the effect of drug polarity.

2. Material and methods

2.1. Materials

FDA, fluorescein, sodium fluorescein (the chemical structures of these substances are shown in Fig. S2, Supplementary Information), polyvinylpyrrolidone (PVP, K30), acetone (>99.5%), dimethyl sulfoxide (DMSO: >99.0%, non fluorescent solvent), sodium chloride (NaCl) and sodium hydroxide (NaOH) were obtained from Wako Pure Chemical Industry (Japan), and used without further purification. Seamless cellulose tubing with a pore size of 50 Å was purchased from Viskase Corporation (USA). Syringe filters with a pore size of 0.22 μm were obtained from Millipore Corporation (USA).

2.2. Animals

Specific-pathogen free male Sprague–Dawley rats, aged 4 to 5 weeks, were obtained from Japan SLC Inc (Japan). All animals were managed in accordance with the rules of the Animal Experiment Committee in Tohoku University.

2.3. Preparation of eye drops

FDA nanoparticle eye drops were prepared using the reprecipitation method [31–33]. The reprecipitation method, which is a solvent displacement method, provides a very simple and versatile way to prepare organic nanoparticle dispersions. The method involves the rapid mixing of a small amount of concentrated stock solution of the target compound dissolved in a good solvent with excess of a poor solvent. In the reprecipitation method, nanoparticles can be successfully prepared without using carriers that are usually necessary for nanoparticle formation. Typically, 200 μl of FDA acetone solution (25 mg/ml) was rapidly injected into a magnetically stirred (1400 rpm) PVP (2%, w/w) containing water solution (10 ml) using a microsyringe at room temperature. Then, water soluble PVP, which is commonly used for current ophthalmic drug formulation as a stabilizer, acted as a stabilizer surrounding the nanoparticles to increase the water stability of the aqueous dispersion of the nanoparticles. The resulting dispersion of nanoparticles in water was dialyzed for 6 h to remove acetone using seamless cellulose tubing. The FDA nanoparticle water dispersion was then filtered by the syringe filter with a pore size of 0.22 μm. The filtered FDA nanoparticle water dispersion was mixed with sterile NaCl water solution (9%, w/w) in a volume ratio of 9:1. Finally, the FDA nanoparticle water dispersion containing NaCl solution (0.9%, w/w) was prepared as eye drops.

FDA microparticle eye drops were prepared as follows. First, FDA powder (25 mg) was dissolved in acetone (1 ml). The solution was evaporated for recrystallization. The recrystallized powders were milled in a mortar. The FDA powder (5 mg) was then mixed with 2% (w/w) PVP water solution (10 ml). Finally, the FDA powder solution was mixed by vortex-induced vibration for 1 min. This was followed by 1 min of sonication to achieve a uniform dispersion of the particles. Only part of the resulting stable dispersion without precipitated aggregates was collected. This FDA microparticle water dispersion was mixed with sterile NaCl water solution (9%, w/w) in a volume

ratio of 9:1 to produce FDA microparticle eye drops containing NaCl (0.9%, w/w).

Fluorescein nanoparticle eye drops were prepared using the reprecipitation method as follows. First, fluorescein (25 mg) was dissolved in DMSO (1 ml), and then 200 μl of this solution was injected into a magnetically stirred (1400 rpm) PVP (2%, w/w) water solution (10 ml). The dispersion was dialyzed for 6 h to remove DMSO, and then passed through a syringe filter (0.22 μm pore size). The filtered solution was mixed with sterile NaCl water solution (9%, w/w) in a volume ratio of 9:1 to produce fluorescein nanoparticle eye drops containing NaCl (0.9%, w/w).

Sodium fluorescein eye drops were prepared as follows. Sodium fluorescein (5 mg) was dissolved in 2% (w/w) PVP water solution (10 ml), and then passed through a syringe filter (0.22 μm pore size). The filtered solution was mixed with sterile NaCl water solution (9%, w/w) in a volume ratio of 9:1 to produce sodium fluorescein eye drops containing NaCl (0.9%, w/w).

The absence of an absorption peak corresponding to the organic solvent used in the reprecipitation method confirmed that it had successfully been removed from the solution. An ultraviolet–visible (UV) absorption spectra measurement (Jasco, V-550) was used for this measurement.

2.4. Calculation of the dye concentration in eye drops

The concentration of dye in the prepared eye drops was calculated by means of measuring the fluorescence intensity of fluorescein in a mixed solution of 1 M NaOH water solution and DMOS (volume ratio is 1:1). In this mixed solution, the concentration of the NaOH was 0.5 M; hereinafter, we refer to this solution as the NaOH–DMSO solution. In the NaOH–DMSO solution, FDA is completely hydrolyzed, which results in generating fluorescein as described the literature [35,37]. A calibration curve was used for estimating the concentration of dye in the eye drops. In our experiment, following the literature [35,37], upon treatment with the NaOH–DMSO solution, FDA nanoparticles were hydrolyzed and green fluorescent fluorescein was produced (Fig. 1 a-ii). The same hydrolysis reaction by the NaOH–DMSO solution treatment was observed when using FDA microparticles (Fig. 1 b-ii). After the hydrolysis reaction, the peak obtained by dynamic light scattering measurement as well as the ζ-potential of the system assigned to the FDA nanoparticles and FDA microparticles was not detectable because of their complete dissolution in the NaOH–DMSO solution. Fluorescence spectra of the fluorescein solution obtained from the eye drops were measured using a fluorescence spectrometer (Hitachi, F-2500). The relationship between the fluorescence intensity (at λ_{max}: 525 nm) of fluorescein and the dye concentration was plotted in calibration curves. The calibration curves used for the measurement of the dye concentration of eye drops is shown in Supplementary Information Fig. S3a.

2.5. Size and morphology evaluation of particles in the eye drops

The size and morphology of FDA nanoparticles and microparticles were estimated through scanning electron microscopy (SEM: JEOL, JSM-6700F). The average size of dispersed FDA nanoparticles and fluorescein nanoparticles was measured by dynamic light scattering (DLS: Malvern Instruments, Zetasizer Nano-ZS). The ζ-potentials of these suspensions were also measured by Zetasizer Nano-ZS.

2.6. Preparation of specimens for quantitative analysis of dye ocular penetration

First, 10 μl of eye drops was administered to the eyes of rats. Then, after a given time (5 min, 30 min, 60 min or 120 min), the rats were euthanized by anesthetic injection. Each eye was washed with excess saline before and after the excision. The dyes in the excised ocular globe were used to calculate the ocular penetration rates of dyes by means of using fluorescence spectrometry.

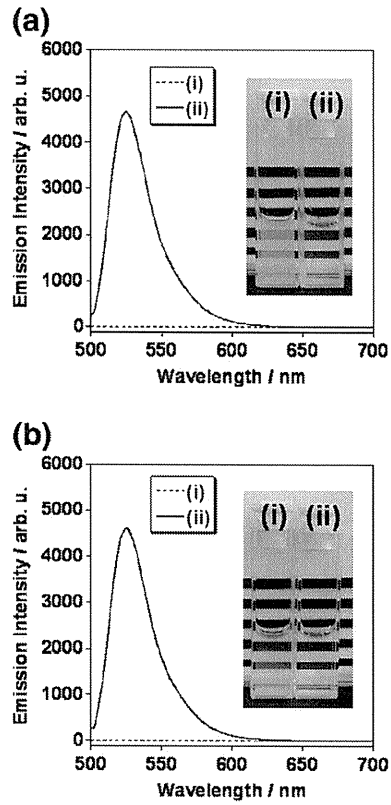

Fig. 1. Fluorescence spectra and photographs of FDA nanoparticles (a) and FDA microparticle (b) aqueous dispersion; before (i) and after (ii) hydrolysis.

For investigation of the dye distributions in the ocular globe, the excised ocular globes were carefully dissected under a microscope to produce eye segments: an anterior eye segment of eye tissue anterior to the equatorial plane that included the crystalline lens, a posterior eye segment containing the sclera and a retina that was peeled off a posterior eye segment.

An additional experiment was performed to reduce the chance of false results due to contamination. For this, FDA nanoparticle eye drops were administered and, after a given time, the eyes were washed with saline before and after excising the ocular globe. The excised ocular globe was immediately frozen in liquid nitrogen, before being dissected as described in the above manner. This technique of dissecting frozen tissue removes the chance of dye contamination caused by the flow of liquid [38].

To extract the dyes from the ocular globes and the divided eye segments, the ocular globes and the divided eye segments were mixed with 2.5 ml and 2 ml of the NaOH–DMSO solution, respectively. This also resulted in the production of fluorescein, as described in the literature [35,37]. These samples in solution were ultrasonicated for several hours (6 h) to extract the dyes from the excised ocular globe and divided eye segments, and these dye solutions were passed through a syringe filter (0.22 μm pore size) to remove residual aggregates of eye tissue.

The solutions obtained from the ocular globe and the anterior eye segments were diluted by a factor of ten before fluorescence spectra measurement because the fluorescence intensity of samples treated with nanoparticle eye drops was high and caused concentration quenching. To dilute the samples, 200 μl of the solutions obtained from the ocular globe and the anterior eye segments was mixed with 1.8 ml of the NaOH–DMSO solution before fluorescence spectra were measured.

To measure the concentration of dye in the anterior chamber, the eye of the euthanized rat was first washed with excess saline before a 30 gage needle was inserted into the anterior chamber through the boundary between the cornea and conjunctiva. The collected anterior chamber humor was mixed with the NaOH–DMSO solution in the volume ratio of 5 μl of aqueous humor per 2 ml of the NaOH–DMSO solution. The solution was then passed through a syringe filter (0.22 μm pore size) and the fluorescence spectra were measured. Ocular globes and eye fragments that were not treated with eye drop administration were used as controls.

2.7. Calculation of ocular penetration rates of dyes

The ocular penetration rates and the dye transition rates (Tables 1–4) of the dyes after administration of eye drops were calculated with the following formula (Eq. (1)):

$$\text{Ocular penetration rate of dye (\%, w/w)} = (\text{the weight concentration of actual dye penetration} \div \text{the weight concentration of the theoretical dye penetration}) \times 100 \quad (1)$$

Here, the "the weight concentration of actual dye penetration" means the real weight concentration of dyes detected in the specimen of the ocular globe and the eye segments, which were calculated using the calibration curve (see, Section 2 Material and methods; Section 2.6); the "the weight concentration of the theoretical dye penetration" means the virtual weight concentration of dyes with an assumption of complete dye transition to the ocular globe after administration of eye drops; i.e., this weight concentration was calculated based on the dye concentration of eye drops (10 μl) that was administered to the eye, and that were calculated using the calibration curve (see, Section 2 Material and methods; Section 2.4).

The calibration curves used for measurement of the ocular penetration rate of the dyes and the concentration of dyes in the anterior humor are shown in Supplementary Information Fig. S3a and S3b, respectively.

For statistical treatment of the data obtained on the ocular penetration rate and the dye distribution in eye segments, t-tests were carried out to investigate the probability (p) of significance. All p values obtained by the t-tests were based on analyzing multiple groups consisting of 5–6 samples for each p value. These p values are shown in Tables 1 to 4.

2.8. Fluorescence and confocal laser fluorescence microscopy observation

For the fluorescence microscopy observation of the ocular surfaces (Fig. 3), eye drops (10 μl) were administered to the eyes of anesthetized rats, and then after a given time, the eyes were observed by fluorescence microscopy (Zeiss, SteREO Lumar. V12). For confocal laser fluorescence microscopy (Figs. 5–7), ocular globes excised from euthanized rats were placed on glass-bottom dishes (35 mm, Corning) with the corneal side on the glass before the cross-section of the cornea was observed directly by confocal laser fluorescence microscopy (Olympus, FV-300). The laser source used in the experiment was an Ar laser with a 488 nm wavelength. A band pass filter (Olympus, BA510IF) was used to remove any excitation leakage. The series of fluorescence images obtained by both fluorescence and confocal laser fluorescence microscopy were confirmed as not being auto fluorescence of the cells and tissues; this was confirmed by comparing the ocular globes without staining dye as a control.

Table 1
Ocular penetration rates (%, w/w) of dyes after the administration of FDA nanoparticle and FDA microparticle eye drops.

Types of eye drops	Time after administration of eye drops			
	5 min	30 min	60 min	120 min
	Mean value of ocular penetration rate (%, w/w)			
FDA nanoparticles	9.00*,†	4.80*,†	3.45*,†	1.32*,†
FDA microparticles	0.18***	0.14**	0.12**	0.09**

Concentration of administered eye drops was 0.17 mg/ml.
Number of samples used for calculating each mean value: n = 6; except FDA microparticles at 5 min: n = 5.
* T test: $p<0.0001$ vs. control.
** T test: $p<0.005$ vs. control.
*** T test: $p<0.05$ vs. control.
† $p<0.0001$ vs. FDA microparticles.

Table 2
Ocular penetration rates of dyes after the administration of fluorescein nanoparticles and sodium fluorescein eye drops.

Type of eye drops	Time after administration of eye drops			
	5 min	30 min	60 min	120 min
	Mean value of ocular penetration rate (%, w/w)			
Fluorescein nanoparticles	0.18**	0.09**	0.10**	0.05**
Sodium fluorescein	0.16*	0.07**	0.07**	0.04**

Concentrations of administered fluorescein nanoparticle eye drops and sodium fluorescein eye drops were 0.29 mg/ml and 0.36 mg/ml, respectively.
Number of samples used for calculating each mean value: n = 6.
* T test: $p<0.0001$ vs. control.
** T test: $p<0.005$ vs. control.

3. Results and discussion

3.1. Evaluation of the size and morphology of FDA nanoparticles and FDA microparticles

FDA nanoparticles were prepared by the reprecipitation method [31–33]. Scanning electron microscopy (SEM) showed that the morphology of FDA nanoparticles prepared by the reprecipitation method was spheroidal (Fig. 2a). Dynamic light scattering (DLS) measurements showed that nanoparticle sizes were monodispersely distributed with an average size of 215 nm and that the ζ-potential of the system was −10 mV (Fig. S4, Supplementary Information). These nanoparticles were stably dispersed in aqueous medium because of a negatively charged ζ-potential as well as stabilizer PVP. These nanoparticles were stably dispersed in aqueous medium as shown in the photograph in Fig. 1 a-i. On the other hand, particles not formed by the reprecipitation method had a poor morphology. SEM showed that these particles were angular rather than spheroidal and that their size distribution spread across several micrometers. These results are shown in Fig. 2b, and the particles are referred to as microparticles in the remainder of this work. For the administration of eye drops to the eyes of rats, nanoparticle and microparticle eye drops were used

Table 3
Localization of dye obtained from each eye segment after administration of FDA nanoparticle eye drops.

Eye segments	Time after administration of eye drops			
	5 min	30 min	60 min	120 min
	Mean value of dye transition rate (%, w/w)			
Anterior eye	7.07*	6.06*	3.16*	1.45*
Sclera	0.04**	0.02*	0.01*	0.01***
Retina	0.02***	–	–	–

Concentration of administered FDA nanoparticle eye drops was 0.28 mg/ml.
Number of samples used for calculating each mean value: n = 6.
* T test: $p<0.0001$ vs. control.
** T test: $p<0.005$ vs. control.
*** T test: $p<0.05$ vs. control.

Table 4
The localization of dye obtained from frozen eye segments after administration of FDA nanoparticle eye drops.

Eye segments	Time after administration of eye drops			
	5 min	30 min	60 min	120 min
	Mean value of dye transition rate (%, w/w)			
Anterior eye	4.70*	3.56*	2.99*	0.78*
Conjunctiva–Sclera	0.31***	0.12**	0.04***	0.02***
Vitreous body	–	–	–	–
Retina	0.01***	–	–	–

Concentration of administered FDA nanoparticle eye drops was 0.42 mg/ml.
Number of samples used for calculating each mean value: n = 6.
* *T* test: $p<0.0001$ vs. control.
** *T* test: $p<0.005$ vs. control.
*** *T* test: $p<0.05$ vs. control.

before hydrolyzation and, therefore, the non-hydrolyzed FDA shows no fluorescence before their administration.

3.2. Fluorescein nanoparticles and sodium fluorescein eye drops

To examine the influence of polarity on the ocular penetration of eye drops, both fluorescein nanoparticles and sodium fluorescein eye drops were prepared for comparison with the FDA eye drops. The polarity of the chemical compound was described using octanol/water partition coefficient, log *P*. The log *P* of fluorescein is 0.61 and that of sodium fluorescein is −0.67 [39,40]. Since the log*P* of FDA is 3.51 [40], fluorescein and sodium fluorescein can be regarded as more hydrophilic than FDA because they have lower partition coefficients. Actually, fluorescein and sodium fluorescein are slightly and highly soluble in water, respectively. The average size of the fluorescein nanoparticles was 14 nm (Fig. S5, Supplementary Information) and sodium fluorescein in solution was molecular in size.

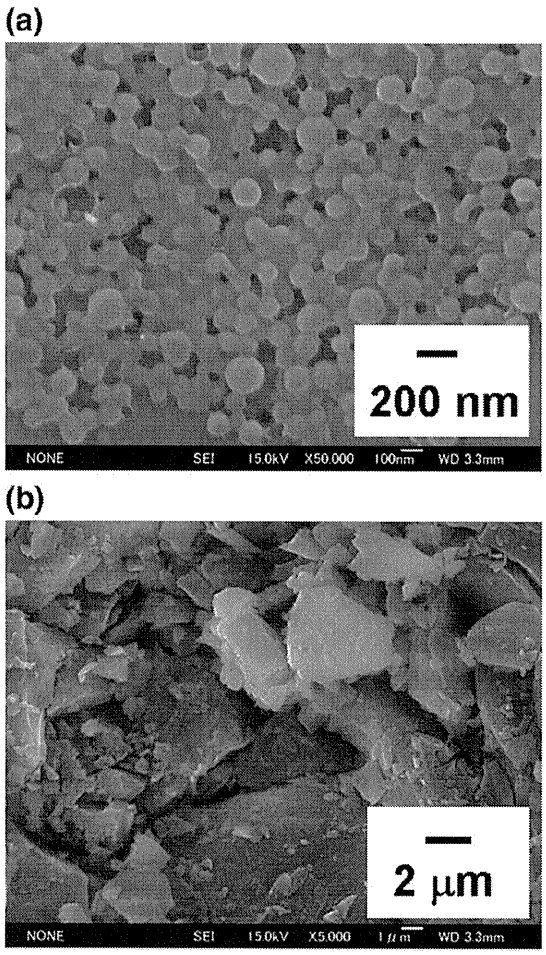

Fig. 2. SEM images of FDA nanoparticles (a) and FDA microparticles (b).

3.3. Fluorescence microscopy observation of ocular surfaces

Ocular surface images after administration of the eye drops are shown in Fig. 3. Fluorescence was not detected in the period from 10 s to 2 min after the administration of FDA nanoparticle eye drops, but was observed after 5 min (Fig. 3a). This fluorescence remained observable after the eye was washed using excess saline (Fig. 3a). In contrast, significant fluorescence was not detected in the ocular globe even at 5 min after the administration of FDA microparticle eye drops (Fig. 3b). Although the concentrations of FDA nanoparticle and FDA microparticle eye drops were the same, these results indicate that the particle size of FDA had a significant effect upon the rate of ocular penetration of the dye.

For both cases, fluorescence was detected at 10 s to 5 min after eye drop administration, but fluorescence was not detected after washing out the eyes with excess saline (Fig. 3c and d). This result indicated the dye in eye drops of fluorescein nanoparticles and sodium fluorescein did not permeate the epithelium. This means that the hydrophilic moieties present in their structure was not preferable for their penetration into the lipophilic corneal epithelium.

Additionally, the observation result using fluorescein eye drops eliminated the chance that the hydrolyzed FDA nanoparticles, which generate fluorescein outside of the ocular globe, entered into the corneal epithelium. Namely, it is clear that the dyes of the FDA nanoparticles were initially taken up by corneal epithelium cells and then the dyes were hydrolyzed inside the cells.

3.4. Quantitative analysis of the ocular penetration rate after administrating eye drops

The ocular penetration rates of FDA nanoparticle and microparticle eye drops were evaluated by quantitative analysis by means of measuring the fluorescence intensity of prepared specimens at a given time after administration of the eye drops (see, Section 2 Material and methods; Section 2.6). The highest fluorescence intensity was observed at 5 min after administering both eye drops (Fig. 4a). Additionally, the fluorescence intensity of FDA microparticle eye drops was less than that of FDA nanoparticles in all measurement times after their administration (Fig. 4b). The fluorescence intensity of both eye drops decreased as time elapsed (Fig. 4b). The temporal ocular penetration rates of these dyes are summarized in Table 1. The ocular penetration rate of dyes in FDA nanoparticles eye drops (9.00% w/w) was several times higher (ca. 50-fold) than that of the FDA microparticles (0.18% w/w) at 5 min after administration (Table 1). This shows that the downsizing of particles from a micrometer to a nanometer scale resulted in achieving high ocular penetration of dyes. This may mean that the dissolution rate of dyes from these particles on the ocular surface was greater for nanoparticles compared with that of microparticles because of a size effect, and then the dyes originating from the nanoparticles permeated into the corneal epithelium. Otherwise, nanoparticles being taken up into the corneal epithelium cells are considered to have occurred in the case of nanoparticle eye drops. The dyes and particles that did not migrate to the ocular globe were washed away from the eye surface by the actions of lacrimation and tear turnover. Similarly, the reason for the reduction of the dye amount observed in the ocular globe over time may be due to the action of aqueous flow in removing the dye and to

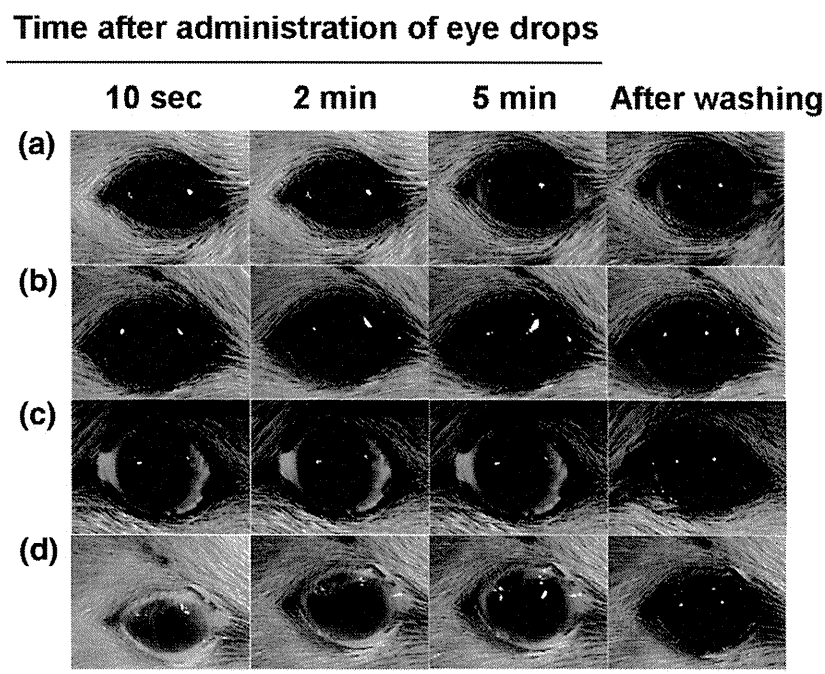

Fig. 3. Fluorescence microscopy images of the ocular surfaces after eye drop administration. The applied eye drops were FDA nanoparticles (a), FDA microparticles (b), Fluorescein nanoparticles (c), and sodium fluorescein (d). Concentration of administered eye drops was 0.47 mM (number of molecules) in each case.

the diffusion of dye into the blood circulation. These mechanisms have been recognized in previous research [11].

The ocular penetration rates of fluorescein nanoparticles and sodium fluorescein were weak during the 2 h following eye drop administration (Table 2 and corresponding graphs in Fig. S6, Supplementary Information). These results are consistent with the existing literature that describes the cornea permeability of chemical compounds according to the log *P*. Since the log *P* of fluorescein and sodium fluorescein is 0.61 and −0.67, respectively, it has been found that compounds with log *P* values of around 2–3 penetrate the cornea more readily [41,42]. Even though, the sizes of fluorescein nanoparticles (ca. 14 nm in size) and sodium fluorescein (molecular in size) were smaller than that of FDA nanoparticles (ca. 215 nm in size), the ocular penetration rate was less than that of FDA nanoparticles. This result means that not only the size but also the polarity of the compound is an important factor for determining the ocular penetration of dyes.

3.5. Confocal laser fluorescence microscopy of the cornea

Since the cornea is a transparent tissue, it is possible to observe a cross section of the tissue using confocal laser fluorescence microscopy. When administrating FDA nanoparticle eye drops, deep cornea penetration of dyes was observed (Fig. 5a; the detailed discussion is in a Section 3.6). For the other types of eye drops studied (i.e., FDA microparticles, fluorescein nanoparticles, and sodium fluorescein), only confocal fluorescence images of surfaces of the superficial corneal epithelium were taken (Fig. 5b–d) and these results showed that the permeation of these dyes through the epithelium was low. Thus, less ocular penetration took place.

3.6. Fluorescence imaging of corneal cross-sections after administrating FDA nanoparticle eye drops

Among the four types of eye drops used in this study (FDA nanoparticles, FDA microparticles, fluorescein nanoparticles, and sodium fluorescein), FDA nanoparticle eye drops were found to have the highest ocular penetration rate. We therefore focused on investigating FDA nanoparticle eye drops. Sixty minutes after the administration of FDA nanoparticle eye drops, a fluorescence image of the corneal cross section was taken that depicted the epithelium, stroma, and endothelium (Fig. 6a). The corresponding fluorescence intensity distribution curve in the cornea and plane view images of each layer are shown in Fig. 6b and Fig. 6c-i, respectively. The depths of plane view images of Fig. 6c-i correspond with the lower-case labels c-i in yellow in Fig. 6a. In the corneal epithelium, the dyes were observed in the cell cytoplasm in the superficial layer (Fig. 6c) and intercellular spaces in the suprabasal and basal layers (Fig. 6d and e). FDA might have been taken up by the corneal epithelium cells in the form of FDA molecules originating from the dissolved nanoparticles on the corneal surface and/or in the form of FDA nanoparticles. It is speculated that the molecular dyes and/or the nanoparticles were hydrolyzed in the cytoplasm of cells in the superficial layer, then the hydrolyzed dyes and/or the nanoparticles having hydrolyzed a surface of fluorescein were exocytosed. These dyes and fluorescent nanoparticles might have passed through the intercellular spaces of the suprabasal and basal layers because their hydrophilic moiety, caused by fluorescein, made it difficult to reenter the cells that were covered by the lipophilic membrane. Fig. 6f and g shows fluorescent dots that may be the aggregation of fluorescent nanoparticles that had hydrolyzed and thus had a fluorescent surface of fluorescein. The sizes of aggregation substances were estimated to be up to several micrometers. For easier viewing, these fluorescent aggregate substances between the basal epithelium layer and stromal layers are enlarged in Fig. 6g and highlighted inside yellow circles. This result indicates the possibility of direct nanoparticle permeation into the corneal epithelium. Since these fluorescent aggregates were trapped in the boundary between the epithelium and stroma (see, lower-case labels f and g in Fig. 6a, and f and g), the hydrophilic fluorescein dyes produced by the hydrolyzed FDA of the nanoparticles might have dominantly permeated through the hydrophilic stroma (Fig. 6h). Then these dyes reached the endothelium (Fig. 6i).

To investigate the details of dye transition from the epithelium to the stroma, a three-dimensional image was taken using the alpha blend method (Fig. 7a). Again, this image shows the passage of

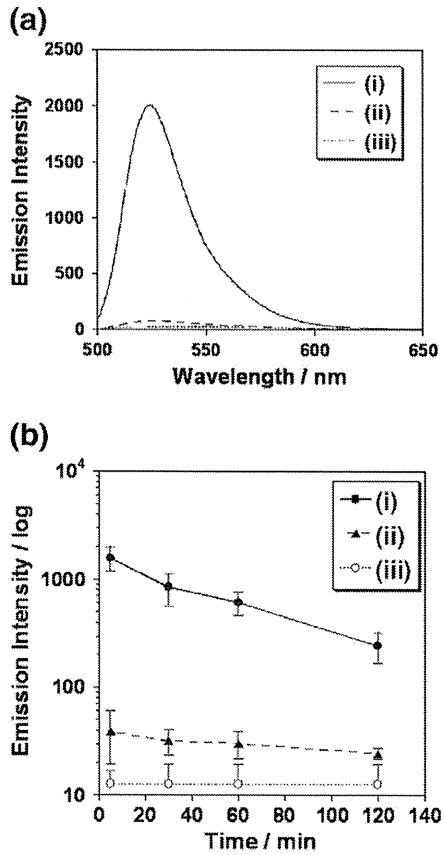

Fig. 4. Emission spectra of dye solution from excised ocular globes at 5 min after eye drop administration (a): FDA nanoparticles (i) and FDA microparticles (ii) eye drops and control (without staining dyes) (iii). Dye transition to the ocular globe at 5, 30, 60, and 120 min after eye drop administration (b): detecting at the λ_{max} (=525 nm) of the florescence spectra for the case of administration of FDA nanoparticles (i) and FDA microparticles (ii) eye drops and control (without staining dyes) (iii); each point value represents the mean ± s.d., and n = 6, except (ii) at 5 min (n = 5).

fluorescent dye through the intercellular spaces between the epithelium. Additionally, fluorescent distributions and fluorescent images of the epithelium (Fig. 7b) revealed that most dyes were absorbed by the superficial layer (Fig. 7b-i) and passed through the intercellular spaces of the suprabasal and basal layers (Fig. 7b-ii and b-iii). The red arrow in Fig. 7b-ii shows a fluorescent cell. This example cell shows that some dyes were taken up by cells in the suprabasal layer. It seems that some dyes and/or nanoparticles might have passed through the tight junctions, and then entered the cell in the suprabasal layer, followed by being hydrolyzed inside the cytoplasm. Although tight junctions work as a good barrier for substances external to the epithelium [43], dye clusters and/or small sized nanoparticles can pass through the pores existing between these tight junctions [43] rather than becoming entrapped in the cells of the superficial layer of the epithelium. However, the exact mechanism for this penetration is still being investigated. Additionally, the cell that took up the dyes and/or nanoparticles in the suprabasal layer were easily observable in the transparent three-dimensional image obtained using the maximum intensity projection method (Fig. 7c, the fluorescent cell is shown by the red arrow). The fluorescent cell in Fig. 7c corresponds with that of Fig. 7b-ii.

Fluorescein dyes produced by hydrolysis of FDA permeated through the hydrophilic stroma, which was confirmed by both the alpha blend method (Fig. 7a) and the maximum intensity projection method (Fig. 7c). These results mean that the formulation of nanoparticles of a hydrolyzable compound can overcome the corneal barrier functions, which consist of the tight junctions of the corneal epithelium as well as the different physicochemical properties of the lipophilic epithelium and the hydrophilic stroma.

At present, there are numerous reports discussing the ocular penetration of dyes, nanoparticles, and drugs [9,14,30,44–51]. However, to the best of our knowledge, this is the first time confocal laser fluorescence microscopy was used to clearly visualize the unique penetration pathway of the compounds consisting of nanoparticles with hydrolyzable dyes through the cornea.

3.7. Dye localization in the ocular globe

After administering FDA nanoparticle eye drops and waiting for a given time, the eyes were washed with saline before and after excising the ocular globe. The excised ocular globe was carefully dissected under a microscope to obtain the anterior segment, conjunctiva, sclera, retina, and vitreous body (see, Section 2 Material and methods; Section 2.6). The ocular penetration rate of the dyes in these fragments was determined by quantitative analysis using fluorescence spectra measurements and calibration curves.

Table 3 shows that almost all the dye was found in the anterior segment (e.g., the ocular penetration rate was 7.07% w/w at 5 min), although some dyes reached the sclera and the retina of the posterior eye segment (corresponding graphs are shown in Fig. S7a–S7c, Supplementary Information). Dye was detected in the retina 5 min after administration of FDA nanoparticle eye drops; however, no significant signal was detected after 30 min.

An additional experiment using a frozen ocular globe was performed to reduce the chance of false results due to contamination (see, Section 2 Material and methods; Section 2.6). A similar trend in the ocular penetration of dyes was observed using this technique. Again, most of the dye was detected in the anterior eye segment (e.g., ocular penetration rate was 4.70% w/w at 5 min), while the remainder was detected in the conjunctiva, sclera and retina (Table 4 and the corresponding graphs in Fig. S8, Supplementary Information). Fig. S8d shows that significant fluorescence in the vitreous body of the posterior eye segment was not detected.

The ocular penetration rate of dyes in the anterior chamber after the administration of eye drops was investigated by measuring the dye concentration in the aqueous humor using the calibration curve (Supplementary Information S3b). As a result, 30 min after the administration of FDA nanoparticle eye drops, the aqueous humor was found to have the highest concentration of the dye (0.56 ± 0.24 μg/ml). The changes in fluorescence intensity and the concentration of dye in the aqueous humor over time are summarized in Table 5 and corresponding graphs are shown in Supplementary Information Fig. S7d.

3.8. Transport of dye to the retina

Drug delivery to the retina using eye drops is an ideal delivery method since administration of drugs to the retina are often limited to oral administration, intravenous injection, and local administration (intravitreal injections/implants and periocular injections). These methods have associated risks of systemic toxicity and infections [52,53]. The anterior chamber of the eye is considered to be the main site at which the pharmacodynamic effects of eye drops take effect in intraocular tissue [12]. However, in this study, the dye might have migrated to the retina through the conjunctiva and sclera, and not through the anterior chamber since the greatest fluorescence intensity in our measurements of the retina was observed at 5 min after eye drop administration (0.02%, w/w; Table 3) and the maximum intensity measured from the anterior chamber was observed after 30 min (0.56 ± 0.24 μg/ml; Table 5 and Supplementary Information Fig. S7d). If the dye passed through the anterior chamber, the maximum fluorescence intensity in the retina should appear 30 min after the administration of